Precision half-life measurement of ^{25}Al

J. Long,[1,*] T. Ahn,[1] J. Allen,[1] D. W. Bardayan,[1] F. D. Becchetti,[2] D. Blankstein,[1] M. Brodeur,[1] D. Burdette,[1] B. Frentz,[1] M. R. Hall,[1] J. M. Kelly,[1] J. J. Kolata,[1] P. D. O'Malley,[1] B. E. Schultz,[1] S. Y. Strauss,[1] and A. A. Valverde[1]

[1]*Department of Physics, University of Notre Dame, Notre Dame, Indiana 46556, USA*

[2]*Physics Department, University of Michigan, Ann Arbor, Michigan 48109, USA*

(Received 20 March 2017; published 12 July 2017)

A new precision half-life measurement of ^{25}Al was conducted using the TwinSol β-counting station at the University of Notre Dame. The new measured value of $t_{1/2}^{\text{new}} = 7.1657(24)$ s is in good agreement with the most recent measurement, while being 3 times more precise. Using these new measurements, an evaluation of the ^{25}Al half-life has been performed, leading to an average half-life of $t_{1/2}^{\text{world}} = 7.1665(26)$ s, which is 5 times more precise than it's predecessor and has a more satisfactory Birge ratio of 1.1. To aid in future measurements of correlation parameters, a new Fermi to Gamow-Teller mixing ratio ρ and correlation parameters for this mixed transition have been calculated assuming the standard model validity using the new world half-life.

DOI: 10.1103/PhysRevC.96.015502

I. INTRODUCTION

Precision measurements provide a key window into the nature of the forces at play in the nucleus. These measurements not only allow for further constraint of a number of theories and models of the nuclear interaction [1] but also provide a test of the electroweak sector of the standard model (SM) [2]. One means of probing the SM is through the unitarity test of the Cabibbo-Kobayashi-Maskawa (CKM) quark-mixing matrix [3]. Currently, the most precise unitarity test is performed by taking the sum of the magnitudes of the squares of the three matrix elements in the top row (V_{ud}, V_{us}, V_{ub}). Among the three elements entering the sum, only V_{ud} and V_{us} play critical roles for the unitarity test [4]. Even though the current best values for these elements are consistent with CKM unitarity [4], there are a number of experimental [5,6] and theoretical efforts [7,8] centered on ensuring the reliability of every component entering into the unitarity test, including the determination of V_{ud} because its extracted value has shifted in the past due to more precise measurements [9].

The V_{ud} element can be determined from four types of decay studies: pion decay, neutron decay, superallowed mixed β decay, and superallowed pure Fermi β-decay transitions [3]. Of these four, studies of superallowed pure Fermi decays currently yield the most precise value of V_{ud} [3]. Despite the high precision achieved from pure Fermi transitions, there is a growing interest to obtain more precise V_{ud} measurements from the other types of decays to test the accuracy of the pure Fermi value [10]. As such, superallowed mixed decays are particularly interesting because they provide another opportunity to test the conserved vector current (CVC) hypothesis [11]. If an apparent violation of the CVC hypothesis is found in mirror transitions, which is respected in pure Fermi transitions, it could be due to unaccounted systematic errors in a given measurement, to inappropriate isospin symmetry-breaking corrections being applied to individual members of the data set, or to new physics beyond the SM. Furthermore, because the same calculation methods are used to determine δ_c, the isospin symmetry-breaking correction, in pure Fermi transitions, measurements in mirror transitions would also make interpretation of the pure Fermi data set more robust.

To extract V_{ud} from either pure Fermi or mirror transitions requires measurements of the half-life, the branching ratio, and the Q_{EC} value [12]. To obtain V_{ud} from the mirror transitions additionally requires the more challenging determination of the Fermi to Gamow-Teller mixing ratio ρ, which is only characterized for five transitions [10]. All five of these nuclei are consistent, respecting the CVC hypothesis, while their average [10] is within 1.3σ from the pure Fermi transition values [3]. The mixing ratio has been derived from measurements of one of the following three correlation parameters: the beta asymmetry parameter A_β, the neutrino asymmetry parameter B_ν, and the beta-neutrino asymmetry angular correlation parameter $a_{\beta\nu}$ [10]. Recent efforts to determine the mixing ratio ρ in mirror transition nuclei include a polarization measurement on ^{37}K in anticipation of a measurement of A_β at the TRINAT experiment of TRIUMF [13]. Another effort is the versatile ion-polarized techniques online (VITO) [14] at ISOLDE, which aims at measuring A_β in ^{35}Ar [15], as well as in ^{21}Na and ^{23}Mg in the future [16]. Likewise, the LPCtrap experiment [17] at the Grand Accelerateur National D'Ions Lourds (GANIL) plans to measure $a_{\beta\nu}$ precisely in ^{19}Ne and ^{35}Ar [18]. Finally a new ion trapping experiment is currently being planned at the Nuclear Science Laboratory (NSL) of the University of Notre Dame [19]. Simultaneously, a new precision half-life measurement program on mirror transitions has also begun at the NSL [20]. As part of these efforts, several new radioactive ion beams are currently being developed and separated using the Twin Solenoid (TwinSol) separator [21]. Of the nuclei most recently produced, ^{25}Al, a nucleus that decays by such a superallowed mixed decay, is of particular interest because its half-life is derived from a series of conflicting measurements, each of which is over 40 years old [12]. Hence, to clarify the disagreement, and provide a more reliable lifetime, a precision half-life measurement on ^{25}Al has recently been performed at the NSL and is reported here.

*jlong10@nd.edu

II. EXPERIMENTAL METHOD

The radioactive ion beam (RIB) of ^{25}Al was produced using transfer reactions in inverse kinematics of a $^{24}Mg^{8+}$ ion beam onto a deuterium gas target via the ^{24}Mg(d,n) reaction. To produce the primary beam, a MgCu-TiH cathode was used in the NSL cesium sputtering ion source (SNICS) to create MgH^- molecules. These negatively ionized molecules were then accelerated in the NSL FN tandem accelerator set to a terminal voltage of 7.5 MV. A thin carbon foil at the center of the tandem high-voltage terminal broke up the molecules while stripping multiple electrons from the Mg beam. A mass-analyzing magnet downstream of the tandem high-voltage terminal was used to select only $^{24}Mg^{8+}$ ions, which were then sent to the RIB production target.

After its production, the $^{25}Al^{10+}$ RIB was separated from the primary beam using the TwinSol system. Then, the beam of ^{25}Al was implanted in a thick tantalum foil in the NSL β-decay counting station [20,22]. The measurement was performed using the same procedure outlined in Ref. [20] except that the primary beam was turned off during the counting phase to avoid the presence of a cumulative background from the γ rays emitted after the annihilation of the e^+ from the implanted ^{25}Al. The beam was deflected by applying a high voltage on a steerer plate upstream from the tandem high-voltage terminal.

The ^{25}Al half-life measurement comprised a series of 32 runs where for each run the photomultiplier tube bias, the discriminator threshold, or the initial decay count rate was varied to probe for any possible systematic effects that would affect the measurement.

III. DATA ANALYSIS

Data analysis followed the well-established and widely used method described in detail in Ref. [23], which was also used for the precision half-life measurement of ^{17}F at the NSL [20]. The fitting procedures were tested against simulated data to ensure accuracy and probe for systematic uncertainties. The data analysis was also performed separately by two different group members to ensure the validity of results. Specific details of the data analysis are presented below.

First the data of a given run were screened for any cycles containing only background counts. These corresponded to a few instances where the primary beam was lost due to an electrical discharge of the tandem high-voltage terminal.

Except for these brief interruptions over the course of a run, the total number of detected counts per cycle varied by at most 39%, due largely to variations of the SNICS output. All runs had cycle durations of 145 s, roughly 20 times the half-life of ^{25}Al. The first eight runs were composed of 20 cycles each, with the remaining 24 runs consisting of 50 cycles each. The data were rebinned from the original 14 500 bins to avoid bins with zero counts, as those may introduce a bias into the fitting procedure (see Sec. III A 1).

The ^{25}Al data were fit using the *summed fit* procedure described in detail in Ref. [23]. Because all runs in this experiment had the same cycle lengths, all the data could be combined together into one data set and fit as a whole.

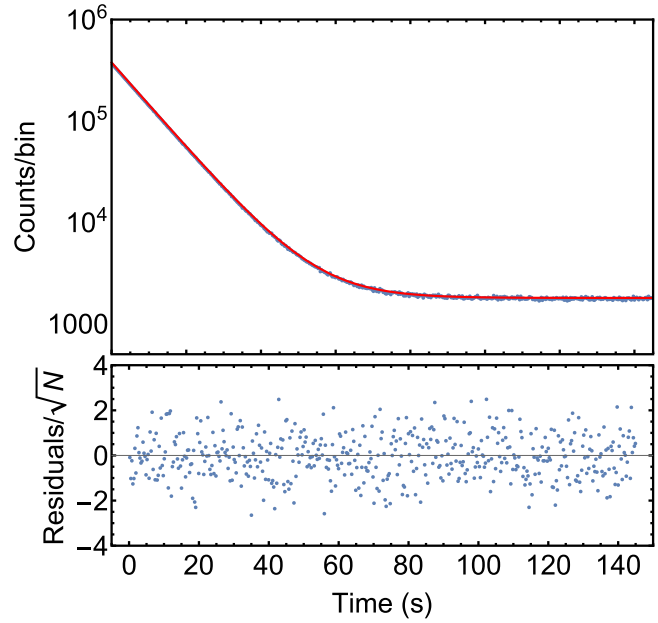

FIG. 1. Summed β-decay curve of all 32 runs. Below are the residuals of the fit divided by the square root of the number of ions in a given bin N. The data have been rebinned to 500 bins.

The number of counts in each bin was corrected for the losses expected from the dead time inherent in the detector system. After this procedure, the following function,

$$r(t) = r_0 e^{-(\ln 2)t/t_0} + b, \tag{1}$$

for the decay rate was used to fit the data, where r_0 is the initial rate, t_0 is the half-life, and b is the background.

The summed fit and corresponding residuals of all the dead-time corrected runs combined and binned to 500 bins is shown in Fig. 1, for which the resulting half-life is 7.1657(23) s. The fit yielded a reduced $\chi^2_\nu = 0.97$ and a mean residual of -0.01 ± 0.98, which together imply that time-dependent systematic effects, such as the presence of unknown contamination or an improper dead-time evaluation, are below the level of our statistical uncertainty.

A. Uncertainty estimation

Several sources of uncertainties in both the measurement and the fitting procedures were explored. These include the influence of binning choice on the outcome of the fit, effects from a possible contaminant, and uncertainty on the dead-time determination.

1. Time binning effects

The effect of rebinning the data was explored using Monte Carlo generated data. In the analysis the binning was varied from the original 14 500 down to 100, at which point the binning becomes too coarse to perform a meaningful fit. To study this effect, 32 runs with $r_0 = 200$ s^{-1} and $b = 3$ s^{-1}, corresponding to the lowest observed rate and a typical background, as well as a half-life of $t_0 = 7.16$ s were used. To get a better statistical uncertainty on the effect of rebinning,

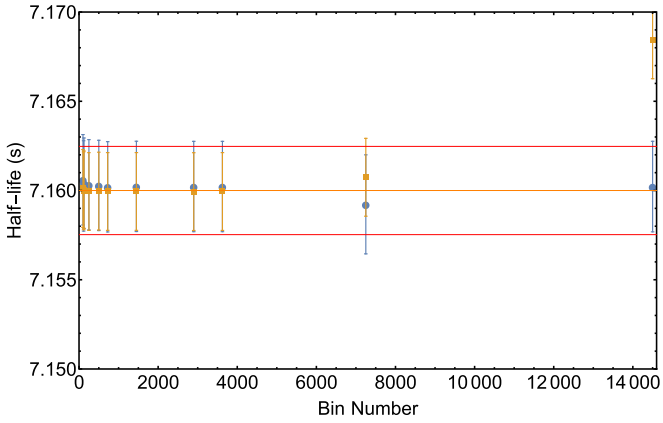

FIG. 2. half-life ^{25}Al fits from Monte Carlo simulated data for various numbers of bins. The blue circles indicate data simulated with a typical background while the orange squares show data simulated with a low background. The central orange line is the true value and the two red outer lines indicate the uncertainty on the weighted average from this work.

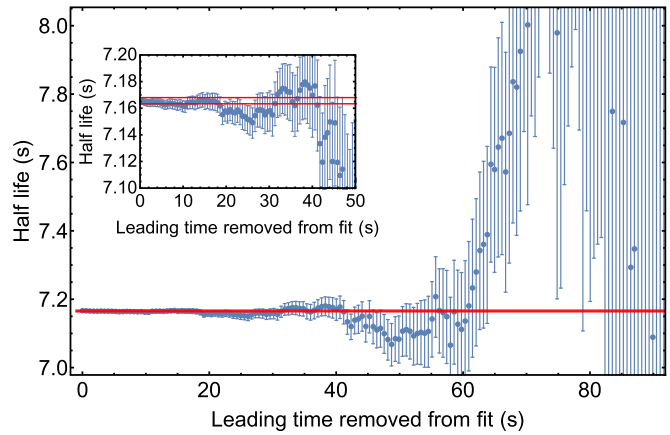

FIG. 3. Fitted half-lives for the total summed data with leading bins removed and the fit performed on the remaining bins. Up to 15 half-lives were removed. The two red horizontal lines indicate the uncertainty on the summed fit without any bin removal.

the Monte Carlo simulations were repeated seven times for each rebinning. The averages of these seven simulation results are shown by the blue circles in Fig. 2. No systematic variations of the fitted half-life with binning within the level of statistical uncertainty of the measurement (red double lines) are observed. Also, the half-life obtained from fitting does not present a bias, within statistical uncertainty, with respect to the half-life used to generate the artificial data indicated by the orange center line. These rebinning effects were also tested for Monte Carlo generated data with a low background count set to $b = 0.3$ s^{-1}. The results of these fits, which are shown by the orange squares in Fig. 2, show that, when the number of time bins is too large, the fit exhibits a bias from many bins with zero counts. Therefore, the data were repartitioned to 500 bins, a choice that does not affect the half-life determination.

2. *Contamination-related considerations*

At the energy used to create ^{25}Al (60 MeV) the only other radionuclide expected to be produced was ^{22}Na. To test the effect of possible ^{22}Na contamination in the beam on the ^{25}Al half-life, Monte Carlo generated data has been fitted using Eq. (1) and also with two exponentials using

$$r(t) = r_0 e^{-(\ln 2)t/t_0} + r_1 e^{-(\ln 2)t/t_1}, \qquad (2)$$

where r_1 and t_1 are the initial rate and the half-life of the contaminant. The artificial data were generated using Eq. (2) where the same r_0 as obtained from the experimental data fit was used while r_1 was set equal to the observed background level. The conservative assumption that all the background comes from the decay of ^{22}Na leads to an upper value estimate on the uncertainty due to the contribution of that decay. Given this assumption, it was found that unaccounted ^{22}Na contamination would result in a relative change in the half-life of 2.3×10^{-6} s at most, so this effect was deemed negligible.

To further investigate the possibility that there could be an unaccounted short-lived contaminant, the leading bins of the total summed histogram were removed one by one and a summed half-life fit was performed on the remaining bins. Up to the first 15 half-lives of the data were removed, corresponding to 98% of all measured counts. Past this point not enough data were left to perform a meaningful fit. The results of this can be seen in Fig. 3, where no time-dependent systematic trends are apparent.

3. *Dead-time uncertainty*

The uncertainty in the dead time $\tau = 30.4(2)$ μs also affects the deduced ^{25}Al half-life. Hence, summed fits over all the runs were performed with a binning of 500 and for the two extreme dead times $\tau = 30.2$ μs and $\tau = 30.6$ μs. The difference of the half-life from each of these fits divided by 2 was taken as a systematic uncertainty. The resulting value, 0.52 ms, was added in quadrature to the statistical counting uncertainty.

4. *Other systematic effects*

Other systematic effects were also explored, including the influence of the photomultiplier voltage, the discriminator threshold, and the beam current. The primary beam current was varied from 2.5 to 15.5 nA; the photomultiplier tube was set to 1505, 1550, 1600, 1605, and 1650 V; and the discriminator was set to 1.02, 1.22, 0.82, and 0.62 V. Runs combining nearly all possible combinations of both photomultiplier tube and discriminator voltages were taken, as shown in Fig. 4. As can be seen in the figure, there are no apparent systematic effects due to these factors.

The half-life was also determined by performing a summed fit for each run individually to probe for systematics. The weighted average of all these values yields a half-life of 7.1651(23) s, with a Birge ratio [12,24] of 0.88. Because this Birge ratio is close to 1 it implies that the fluctuations in the data set are statistical in nature. This half-life value is also in good agreement with the half-life result from the summed fit.

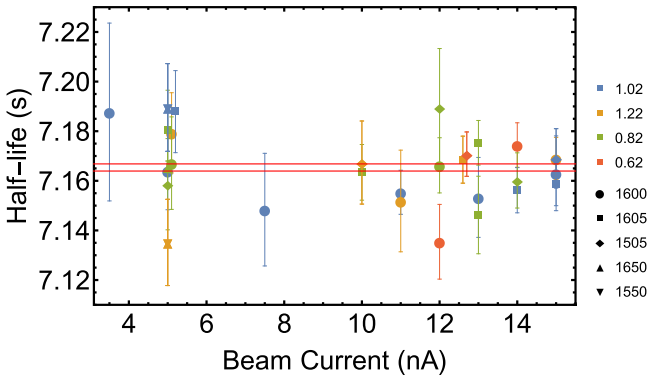

FIG. 4. Plot of the half-lives of ^{25}Al vs the beam current for each run. The point color notates the discriminator voltage and the point shape notates the photomultiplier tube voltage for each run. The red double lines represent the 1σ uncertainty on the weighted average of the individual half-lives.

Finally, adding the statistical uncertainty on the half-life of 2.3 ms with the uncertainty due to the dead-time determination of 0.52 ms yields an overall uncertainty of 2.4 ms.

IV. ^{25}Al HALF-LIFE

The new ^{25}Al half-life measurement of 7.1657(24) s is within 1.4σ of the previous world value of 7.183(12) s while being the most precise measurement to date. With the new lifetime from this work, we also reevaluated the world data. The same procedure as outlined in Ref. [25] was used. Two measurements used to calculate the previous world value [26,27] were rejected because least-squares fitting was used in those analyses. In addition, the oldest ^{25}Al [28] value was removed from the new evaluation due to its uncertainty being over 10 times larger than the most recent measurement, as per the criteria used by Hardy and Towner [25] and the Particle Data Group [29]. Thus only the 1975 measurement [30] was used to calculate the new world value. The two values used to find the new world value are shown in blue in Fig. 5, while the rejected measurements are in red. A weighted average yields a half-life of 7.1665(23) s. The Birge ratio of the world data went from 1.9 down to 1.1 with the new measurement. Using the practices from Refs. [25,29] and scaling the uncertainty by the Birge ratio gives a ^{25}Al half-life value of 7.1665(26) s, a reduction on the uncertainty of the world half-life by a factor of 5. This new world average is shown by the red band in Fig. 5.

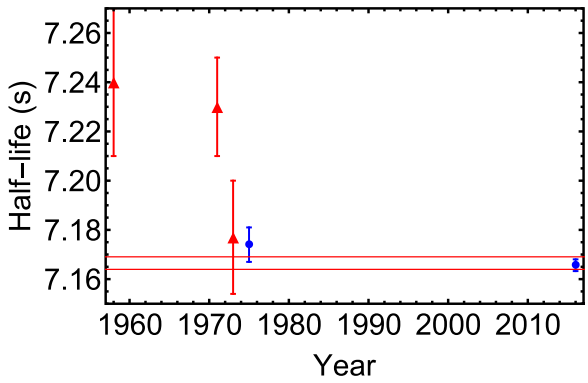

FIG. 5. half-lives ^{25}Al [30] considered in the evaluation of the new world value. The triangle points colored red were included in the old world value but were removed from our evaluation. The scaled uncertainty on the overall ^{25}Al half-life of 7.1665(26) s is represented by the red band.

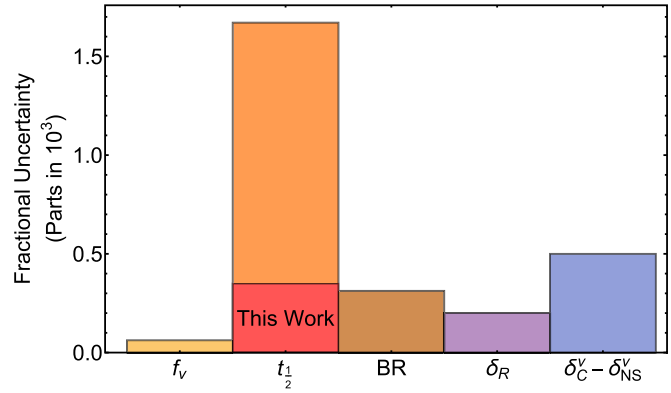

FIG. 6. The relative uncertainty for quantities needed to calculate $\mathcal{F}t^{\text{mirror}}$. The f_v value was calculated from the Q_{EC} value.

V. DISCUSSION

The ^{25}Al half-life is one of three experimental quantities needed to calculate the ft value for that $T = 1/2$ mixed transition, the others being the Q_{EC} value and the branching ratio. Prior to the new half-life measurement the Q_{EC} value of the ^{25}Al decay had been measured more precisely and accurately using a Penning trap [31], yielding a value of $Q_{\text{EC}} = 4276.805(45)$ keV. Using the Q_{EC} value from Ref. [31] and the parametrization from Ref. [32], a value of $f_v = 508.520(32)$ was calculated. Then using the electron-capture fraction $P_{\text{EC}} = 0.079$, the branching ratio 99.151(31)% from Ref. [12], the Q_{EC} value from Ref. [31], the theoretical corrections $\delta_R' = 1.475(20)$, and $\delta_C^V - \delta_{NS}^V = 0.52(5)$ from Ref. [12], the relative uncertainties for these values are summarized in Fig. 6. The $\mathcal{F}t^{\text{mirror}}$ values were calculated using both the half-lives from Ref. [12] and the new world value. The half-life from this work changes the $\mathcal{F}t^{\text{mirror}}$ value by 8.5 s while being 2.5 times more precise. Using this $\mathcal{F}t^{\text{mirror}}$ value, we can extract a SM predicted value for the mixing ratio ρ using [12]

$$\mathcal{F}t^{\text{mirror}} = \frac{2\mathcal{F}t^{0^+\to 0^+}}{1 + \frac{f_A}{f_V}\rho^2}, \tag{3}$$

where $\mathcal{F}t^{0^+\to 0^+} = 3072.27(72)$ s [4] is the average value of the 14 most precisely known pure Fermi $0^+ \to 0^+$ superallowed transitions and f_A is the axial-vector part of the statistical rate function. f_A was evaluated using the parametrization found in Ref. [32] and found to be 520.583(32). Using this new SM predicted value for ρ, the measurable parameters a_{SM}, A_{SM}, and B_{SM} were calculated assuming that the ^{25}Al mirror transition obeys the standard model. All these values are given in Table I. The more precise lifetime of ^{25}Al results

TABLE I. Values for various parameters of relevance for determining V_{ud} from the ^{25}Al mirror transition. The Q_{EC} value from Ref. [31] was used in the calculations.

Parameter	This work	With previous $t_{1/2}$
$t_{1/2}$	7.1665(26) s	7.182(12) s
$f_v t$	3678.4(18) s	3686.9(63) s
$\mathcal{F}t^{\text{mirror}}$	3713.3(26) s	3721.8(66) s
ρ	−0.7997(20)	−0.7974(26)
a_{SM}	0.4799(16)	0.4817(21)
A_{SM}	0.93594(81)	0.9350(10)
B_{SM}	0.71303(12)	0.71289(16)

in an improvement of ≈25% on the uncertainty in the various correlation parameter estimates.

VI. OUTLOOK

A precision half-life measurement of ^{25}Al was performed at the NSL of the University of Notre Dame using a RIB from TwinSol. The new half-life of 7.1657(24) s results in a 5 times more precise world average. The $f_v t$ value uncertainty is still dominated by the half-life so more precision measurements are needed. Finally, to test the CVC hypothesis and to extract a value for V_{ud}, an experimental measurement of the mixing ratio ρ is required. To measure ρ for ^{25}Al and other nuclei, a Paul trap is currently being planned at the Nuclear Science Laboratory of the University of Notre Dame [19].

ACKNOWLEDGMENT

This work was supported by the National Science Foundation (NSF) under Grants No. PHY-1419765, No. PHY-1401343, and No. PHY-1401242.

[1] M. Brodeur, T. Brunner, C. Champagne, S. Ettenauer, M. J. Smith, A. Lapierre, R. Ringle, V. L. Ryjkov, S. Bacca, P. Delheij, G. W. F. Drake, D. Lunney, A. Schwenk, and J. Dilling, Phys. Rev. Lett. **108**, 052504 (2012).
[2] N. Severijns and O. Naviliat-Cuncic, Annu. Rev. Nucl. Part. Sci. **61**, 23 (2011).
[3] J. C. Hardy and I. S. Towner, Rep. Prog. Phys. **73**, 046301 (2010).
[4] J. C. Hardy and I. S. Towner, Phys. Rev. C **91**, 025501 (2015).
[5] K. Gulyuz, G. Bollen, M. Brodeur, R. A. Bryce, K. Cooper, M. Eibach, C. Izzo, E. Kwan, K. Manukyan, D. J. Morrissey, O. Naviliat-Cuncic, M. Redshaw, R. Ringle, R. Sandler, S. Schwarz, C. S. Sumithrarachchi, A. A. Valverde, and A. C. C. Villari, Phys. Rev. Lett. **116**, 012501 (2016).
[6] M. R. Dunlop *et al.*, Phys. Rev. Lett. **116**, 172501 (2016).
[7] W. Satuła, J. Dobaczewski, W. Nazarewicz, and T. R. Werner, Phys. Rev. C **86**, 054316 (2012).
[8] A. Bazavov *et al.* (Fermilab Lattice and MILC Collaborations), Phys. Rev. Lett. **112**, 112001 (2014).
[9] J. C. Hardy and I. S. Towner, Phys. Rev. C **79**, 055502 (2009).
[10] O. Naviliat-Cuncic and N. Severijns, Phys. Rev. Lett. **102**, 142302 (2009).
[11] R. P. Feynman and M. Gell-Mann, Phys. Rev. **109**, 193 (1958).
[12] N. Severijns, M. Tandecki, T. Phalet, and I. S. Towner, Phys. Rev. C **78**, 055501 (2008).
[13] B. Fenker *et al.*, New J. Phys. **18**, 073028 (2016).
[14] M. Stachura *et al.*, Nucl. Instr. Meth. Phys. Res., Sect. B **376**, 369 (2016).
[15] P. H. Velten, M. Bissell, N. Neyens, G. Severijns, and W. Gins, Report No. CERN-INTC-2014-062/INTC-P-426, 2015.
[16] N. Severijns, G. Neyens, and M. Bissell, Report No. CERN-INTC-2013-013/INTC-O-017, Sec. 2.2.3, p. 19, 2013, https://cds.cern.ch/record/1551750/files/INTC-O-017.pdf.
[17] G. Ban, D. Durand, X. Fléchard, E. Liénard, and O. Naviliat-Cuncic, Ann. Phys. **525**, 576 (2013).
[18] X. Fabian *et al.*, EPJ Web Conf. **66**, 08002 (2014).
[19] M. Brodeur, J. Kelly, J. Long, C. Nicoloff, and B. Schultz, Nucl. Instr. Meth. Phys. Res., Sect. B **376**, 281 (2016).
[20] M. Brodeur, C. Nicoloff, T. Ahn, J. Allen, D. W. Bardayan, F. D. Becchetti, Y. K. Gupta, M. R. Hall, O. Hall, J. Hu, J. M. Kelly, J.J. Kolata, J. Long, P. O'Malley, and B. E. Schultz, Phys. Rev. C **93**, 025503 (2016).
[21] F. Becchetti, M. Lee, T. O'Donnell, D. Roberts, J. Kolata, L. Lamm, G. Rogachev, V. Guimarães, P. DeYoung, and S. Vincent, Nucl. Instr. Meth. Phys. Res., Sect. A **505**, 377 (2003).
[22] T. Ahn *et al.*, Nucl. Instr. Meth. Phys. Res., Sect. B **376**, 321 (2016).
[23] V. Koslowsky, E. Hagberg, J. Hardy, G. Savard, H. Schmeing, K. Sharma, and X. Sun, Nucl. Instr. Meth. Phys. Res., Sect. A **401**, 289 (1997).
[24] G. F. Grinyer *et al.*, Phys. Rev. C **71**, 044309 (2005).
[25] J. C. Hardy and I. S. Towner, Phys. Rev. C **71**, 055501 (2005).
[26] F. Jundt, E. Aslanides, B. Fride, and A. Gallmann, Nucl. Phys. A **170**, 12 (1971).
[27] I. Tanihata, T. Minamisono, A. Mizobuchi, and K. Sugimoto, J. Phys. Soc. Jpn. **34**, 848 (1973).
[28] T. Muller, E. Gelsema, and P. Endt, Physica **24**, 577 (1958).
[29] J. Beringer *et al.* (Particle Data Group), Phys. Rev. D **86**, 010001 (2012).
[30] G. Azuelos and J. E. Kitching, Phys. Rev. C **12**, 563 (1975).
[31] L. Canete *et al.*, Eur. Phys. J. A **52**, 124 (2016).
[32] I. S. Towner and J. C. Hardy, Phys. Rev. C **91**, 015501 (2015).